



A K-NN-Driven Multilateration Approach for Improved Aircraft Positioning

Varsha Reddy Manda¹ • Supraja Reddy Ammana*¹,
Mahesh Chilaka² • Venkata Ratnam Devanaboyina³

¹Department of ECE, Chaitanya Bharathi Institute of Technology (CBIT), Hyderabad, India

²Kalaburagi Airport, Airports Authority of India (AAI), Karnataka, India

³Department of ECE, Koneru Lakshmaiah Education Foundation, Guntur 522302, India

Received: 05 04 2025; Accepted: 04 08 2025

Available: 28 02 2026

Abstract: For safe and efficient air traffic management, the Air Traffic Control (ATC) should know the precise location of aircraft. Aircraft usually report their positions to ATC using an advanced location-based service known as Automatic Dependent Surveillance–Broadcast (ADS-B). The location of aircraft without position-reporting capabilities is determined using complementary localization methods. A key challenge with traditional positioning techniques, such as multilateration using Time Difference of Arrival (TDOA), is that they involve solving non-linear equations, which require a precise initial position estimate. In this paper, we propose a novel method for aircraft localization that integrates a traditional positioning technique (multilateration) with data-driven learning using the K-Nearest Neighbors (K-NN) algorithm. The K-NN regression model provides a more realistic initial guess of the aircraft’s position. The results were validated against the actual aircraft positions provided by the OpenSky Network, and the proposed technique demonstrated a 2D root-mean-square error of 39.4 m. This work has significant potential for real-world applications in air traffic management, contributing to safer and more precise aircraft positioning.

Keywords: K-NN, multilateration, aircraft Localization, TDOA.

*Corresponding author.

E-mail address: suprajareddy_ece@cbit.ac.in (S.R. Ammana).

Peer Review under the responsibility of Universidad Nacional Autónoma de México.

1. Introduction

Air traffic control (ATC) is a critical service for managing air traffic and is often considered the pillar of the modern aviation industry. Globally, the number of passenger aircraft is gradually increasing. Over the next twenty years, analysts predict a 5% annual increase in manned aircraft operations. Furthermore, it is expected that by 2035, approximately 250,000 Unmanned Aerial Vehicles (UAVs) will enter the United States' airspace and coexist with manned aircraft (Pan et al., 2019). Consequently, it is essential to develop efficient algorithms capable of accurately determining an aircraft's location in terms of latitude, longitude, and altitude. To achieve this while maintaining operational safety and efficiency, modernization of existing ATC technologies is crucial. The disappearance of Malaysia Airlines Flight 370 underscores the need for more robust methods of aircraft position estimation (Zweck, 2016). Widely adopted positioning techniques include radar, Multilateration (MLAT), and Automatic Dependent Surveillance–Broadcast (ADS-B). Among these, radar-based positioning is the oldest, while ADS-B represents a more modern approach.

Radar systems typically take 4 to 12 seconds to update an aircraft's position and suffer from limited coverage. In contrast, ADS-B enables an aircraft to obtain its position from a Global Navigation Satellite System (GNSS) and broadcast this information to ground stations. These position reports are then transmitted to ATC automation systems for real-time display on air traffic controllers' screens. The ADS-B technique requires updated avionics equipment to transmit and receive ADS-B signals; however, these signals are vulnerable to spoofing and jamming (Rayapu et al., 2017).

To reliably receive ADS-B signals within the intended coverage area, a network of ground stations (receivers or sensors) is typically deployed. Based on the information collected by this network, one of the most widely used methods—Multilateration (MLAT)—can be applied to determine an aircraft's position (Darabseh et al., 2020; Monteiro et al., 2015). Multilateration estimates an object's position by accurately computing the Time Difference of Arrival (TDOA) of signals transmitted by the object and received by three or more ground stations. A detailed description of the multilateration technique is provided in Section 2.1.

Strohmeier et al. (2018) proposed a grid-based localization approach using the K-Nearest Neighbors (K-NN) algorithm. Adesina et al. (2019) conducted a comparative

analysis of localization techniques, including traditional TDOA, Support Vector Regression (SVR), and Deep Neural Networks (DNN). Rayapu et al. (2017) presented a purely multilateration-based hyperbolic positioning method using a minimum of three receivers. Figuet et al. (2020) proposed a hybrid technique that combines multilateration and machine learning for enhanced aircraft localization. In their work, the authors utilized the Levenberg–Marquardt algorithm implemented in SciPy to optimize non-linear equations for estimating aircraft latitude, longitude, and applied a Gradient Boosting regression model to estimate altitude.

In this study, the Euclidean distance serves as the core measure for evaluating the similarity between observed and reference TDOA values, which aligns directly with the fundamental mechanism of the K-NN algorithm. Due to this inherent compatibility, K-NN proves particularly effective for this application. This choice is further supported by previous research. Wang et al. (2025) applied a weighted variant of K-NN for hybrid TOA, AOA, and RSS-based fingerprinting and demonstrated strong performance with minimal model complexity compared to advanced regression techniques. Yu et al. (2014) demonstrated that K-NN performs effectively for RF signal localization, leveraging Euclidean distance to achieve robust and accurate position estimates.

Based on these insights, this paper adopts a novel approach that integrates MLAT with the K-NN algorithm for aircraft localization. The K-NN model provides an initial estimate of the aircraft's latitude and longitude, which is then used to solve the nonlinear equations in the multilateration process to improve positional accuracy. This method remains effective even with only a minimal number of receivers (as few as three), making it both practical and scalable for real-world deployment.

2. Theoretical Background

The main focus of this paper is to improve multilateration efficiency by leveraging a simple machine learning algorithm. This section provides a brief overview of the working principles of MLAT and TDOA.

2.1 Multilateration

MLAT is a time-tested technology originally developed for military applications to determine aircraft locations. It uses TDOA and is particularly effective for tracking aircraft that do not actively broadcast their positions. The basic working principle of MLAT is illustrated in Figure 1.

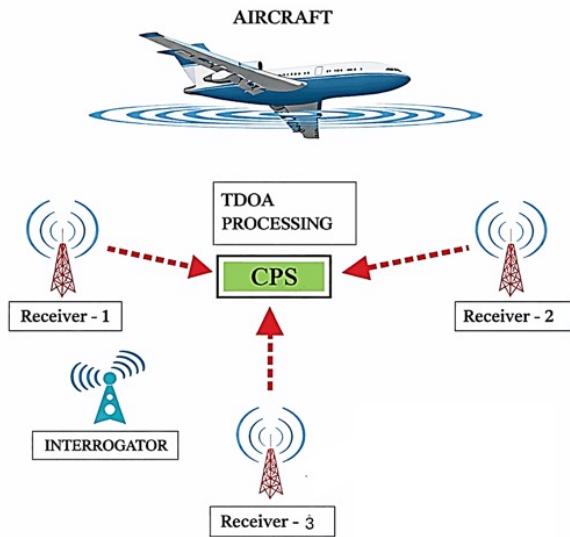


Figure1. MLAT Operation.

Each aircraft is equipped with a transponder, whose primary function is to generate and transmit a reply signal in response to an interrogating signal sent by an interrogator. The interrogator may be a ground station in the MLAT receiver network or a secondary surveillance radar. All interrogating signals are transmitted at 1030 MHz, and replies are sent at 1090 MHz. There are three transponder modes: Mode A, Mode C, and Mode S. Modes A and C transmit a reply pulse only when an interrogating pulse is received, while Mode S transponders with squitter functionality generate and transmit spontaneous reply signals once every second. ADS-B signals are also transmitted twice per second without requiring any interrogation (Strohmeier et al., 2015). Regardless of the transponder mode, ground stations in the MLAT network continuously listen to aircraft signals on 1090 MHz and time-stamp their arrival. These time-stamped signals are sent to a Central Processing System (CPS), where TDOA is applied to estimate the aircraft's position (Wu et al., 2019).

MLAT requires at least three ground stations, or four if altitude information is to be computed. These ground stations are strategically placed at known, fixed locations. Implementing MLAT does not require any upgrades to the aircraft's avionics equipment and can also be used to cross-verify the accuracy of reported positions. MLAT plays a significant role in monitoring aircraft on airport surfaces; today, it forms an integral part of Advanced Surface Movement Guidance and Control Systems (A-SMGCS),

which are being deployed at several international airports worldwide (Rayapu et al., 2017).

2.2 Time Difference of Arrival

The TDOA method is commonly used to geolocate RF sources. It requires three or more receivers, positioned at known locations, that are capable of detecting the desired signal. Each incoming signal is time-stamped, and the differences in arrival times between receivers are calculated.

Consider three receivers — Receiver-1, Receiver-2, and Receiver-3 — located at known coordinates (x_1, y_1) , (x_2, y_2) and (x_3, y_3) respectively. All receivers share a common clock and are time-synchronized. For mathematical simplicity, Receiver-1 is chosen as the reference. As an aircraft enters the coverage area, its signal is detected by the receivers at different times based on their relative positions. Each receiver time-stamps the incoming signal and forwards the data to a central processor. Let t_1 , t_2 , and t_3 denote the arrival times of the signal at Receiver-1, Receiver-2, and Receiver-3, respectively, and let c represent the propagation speed (i.e., the speed of light). Let (x, y) be the unknown coordinates of the aircraft. The TDOA values are then computed as shown in Equations 1 and 2 (Liu et al., 2018; Ran et al., 2016; Tekdas & Isler, 2010; Weinstein, 1982; Xu et al., 2006).

$$TDOA_{2,1} = TOA_2 - TOA_1 \tag{1}$$

$$TDOA_{3,1} = TOA_3 - TOA_1 \tag{2}$$

Where,

$TDOA_{2,1}$ = Time difference of arrival of signal between receiver 1 and 2

$TDOA_{3,1}$ = Time difference of arrival of signal between receiver 3 and 1

TOA_1 = Time of arrival of signal at receiver 1

TOA_2 = Time of arrival of signal at receiver 2

TOA_3 = Time of arrival of signal at receiver 3

If Δt_1 represent $TDOA_{2,1}$, the range difference (Δd_1) between the aircraft and Receiver-1, Receiver-2 is given by Equation 3,

$$\begin{aligned}
 c * \Delta t_1 &= \Delta d_1 \\
 &= \sqrt{(x_2 - x)^2 + (y_2 - y)^2} \\
 &\quad - \sqrt{(x_1 - x)^2 + (y_1 - y)^2}
 \end{aligned} \tag{3}$$

Similarly, another range difference equation between the aircraft and Receiver-1, Receiver-3 is given by Equation 4,

$$\Delta d_2 = \sqrt{(x_3 - x)^2 + (y_3 - y)^2} - \sqrt{(x_1 - x)^2 + (y_1 - y)^2} \quad (4)$$

The (x,y) coordinates of the aircraft are obtained by solving Equations 3 and 4. Due to the significant nonlinearity of these equations, determining the location is somewhat challenging. These nonlinear equations form hyperbolic contours. When two such hyperbolas are plotted, they intersect at a single point, which corresponds to the aircraft's true location. This method is known as hyperbolic positioning, a variant of multilateration (Lee, 1975; Torrieri, 1984). To solve these nonlinear equations, both iterative and algebraic approaches — such as Taylor series expansion, weighted least squares, and the Newton–Raphson method — have been reported in the literature (Chen et al., 2018; Ho et al., 2007; Jin et al., 2018; Lui et al., 2009; Peng et al., 2020; Shen et al., 2012; Torrieri, 1984).

These nonlinear optimization techniques converge on a best-fit solution that satisfies the mathematical constraints. However, to initiate the iterative process, an initial guess is required—specifically, an estimate of the aircraft's latitude and longitude. In this context, machine learning algorithms can be trained to analyze historical data and provide more accurate initial estimates, thereby improving convergence speed and accuracy.

Integrating machine learning algorithms with traditional positioning techniques can enhance performance and improve accuracy. This study aims to improve multilateration precision by employing a K-NN regression model to provide a more accurate initial estimate of the aircraft's position.

3. Data Statistics

Real-time ADS-B data is sourced from the OpenSky Network, a non-profit organization based in Switzerland that provides open access to flight monitoring data. The ADS-B signals are collected through a network of 716 time-synchronized receivers deployed at predefined geographic locations. These receivers timestamp the signals transmitted by aircraft and forward them to the OpenSky

Network server, where the data is stored for further analysis. Table 1 provides a brief description of each field present in the ADS-B dataset (Figuet et al., 2020).

Table 1. Description of data fields present in ADS-B data set.

Data Field	Description
Id	Unique identifier of each received signal
Time at server	Time stamp (s) indicating when the OpenSky server received the information.
Aircraft	Unique aircraft identifier assigned to each aircraft.
Latitude	Reported aircraft latitude (degrees)
Longitude	Reported aircraft longitude (degrees)
geoAltitude	Reported aircraft altitude (m)
baroAltitude	Barometric altitude (based on on-board aircraft equipment) reported by aircraft (m)
numMeasurements	Number of receivers that detected the same aircraft position (latitude, longitude, and geometric altitude) at different time instants.
measurements	JSON string containing the station identifier, time stamp of signal reception (ns), and received signal strength.

The ADS-B dataset obtained from the OpenSky Network is available in CSV format, and a sample is shown in Figure 2. Each row in the dataset represents the position of an aircraft as reported by different ground stations at various timestamps.

As the receivers in the network are placed at predefined locations, the OpenSky Network also provides information about each receiver's latitude, longitude, and altitude in CSV format, as shown in Figure 3. The data field serial is a unique identifier assigned to each receiver.

In the ADS-B dataset used for this work, there are 1,048,575 data records corresponding to 1,207 unique aircraft. It is observed that the OpenSky Network has not included position information for some of these aircraft; specifically, 57,099 records lack position data and require estimation.

id	timeAtServer	aircraft	latitude	longitude	baroAltitude	geoAltitude	numMeasurements	measurements
1	0	109	51.60674	-0.20485	2590.8	2590.8	2	[[532,969020406,89],[216,969100125,23]]
2	0	840	51.28078	-0.69862	8907.78	8846.82	2	[[532,976779968,72],[216,976836703,32]]
3	0	1819	51.35457	-0.30418	5791.2	5722.62	2	[[532,980862171,91],[294,980898968,101]]
4	0.00099993	719	46.95305	14.28997	10972.8	10820.4	3	[[149,957322046,48],[143,957512484,102],[133,956973187,76]]
5	0.00300002	2738	38.85147	-8.87866	4343.4	4358.64	2	[[136,933518187,50],[569,933869875,28]]
6	0.00300002	2300	52.41987	5.51702	10972.8	10797.54	2	[[247,973965687,28],[134,974070546,29]]
7	0.00499988	1342	48.73084	9.119592	10972.8	10843.26	2	[[598,970663515,170],[460,970936427,23]]
8	0.0079999	95	49.10316	8.094529	4442.46	4373.88	2	[[663,986345937,43],[460,986043372,22]]

Figure 2. Sample of real-time ADS-B data taken from open sky network.

serial	latitude	longitude	height	type
1	46.68107	7.665313	680.9232	SBS-3
2	40.33704	-3.77021	735.7872	SBS-3
3	0	0	0	SBS-3
4	47.14306	7.243889	550.164	SBS-3
5	52.35646	4.952216	0	dump1090
6	47.1742	8.5247	0	Radarcape
7	38.89867	22.43072	60.0456	Radarcape
8	47.84991	12.12935	137.16	SBS-3
9	45.41094	11.88753	0	Radarcape
10	47.40017	8.63068	430.6824	Radarcape

Figure 3. Sample of the receiver’s location data from the OpenSky network.

4. Methodology

From the available dataset, each aircraft record with an unknown position is included in the testing dataset, while records with known positions are included in the training dataset. The testing dataset contains all the data fields listed in Table 1, except for latitude, longitude, and geo-altitude, which are set to zero and need to be estimated. The methodology used for implementing K-NN-based multilateration is shown in Figure 4.

From the testing dataset, data corresponding to the Time of Arrival (TOA) of aircraft signals (time at the server) is used, and TDOA is calculated using one receiver as the reference receiver (following the procedure in Section 2.2). A similar procedure is carried out on the training dataset for the same combination of receivers, where for every record in the training dataset, one receiver is taken as the reference and the corresponding TDOA is computed. The K-NN algorithm is fitted on the training dataset to learn the underlying patterns and relationships within the data. For the corresponding test data record, the K nearest neighbors from the training data are used, and

the mean latitude and longitude of these K neighbors are calculated. The latitude and longitude thus obtained are taken as the initial guess for the corresponding test data record, and equations are formed based on the TDOA mathematical model. A Python nonlinear optimization function (fmin_l_bfgs_b) is used to solve the TDOA equations and estimate the aircraft’s position. This procedure is repeated for each record in the testing dataset.

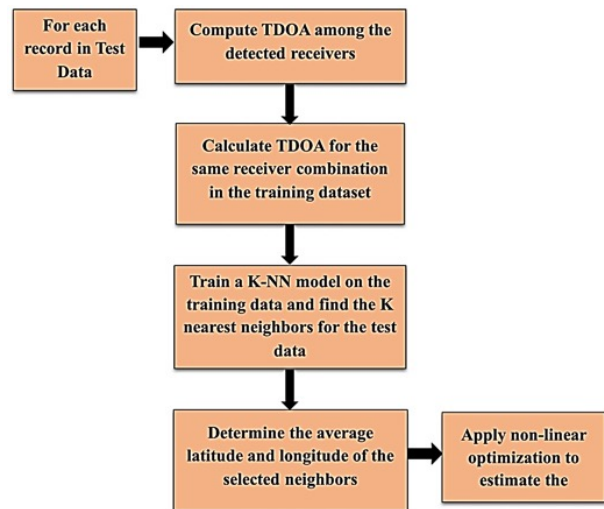


Figure 4. Flow graph of the position estimation procedure.

5. Results and Discussion

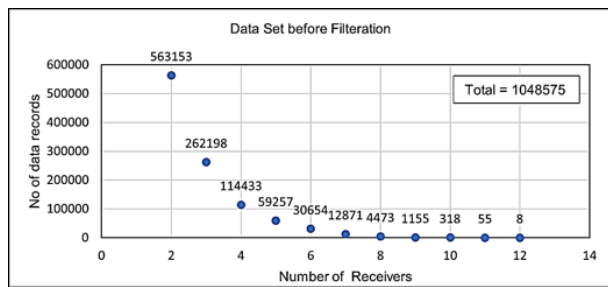
5.1 Data Pre-Processing

According to the statistical data, 57,099 of 1,048,575 records had unknown aircraft positions. These incomplete records correspond to 32 different aircraft observed at various points during their flights. Since MLAT standards require a minimum of three receivers to estimate a position, data fields with a numMeasurements value of 2 are

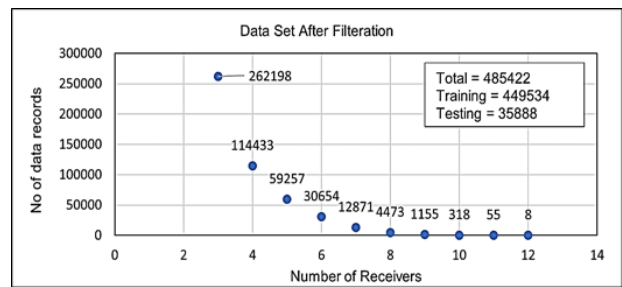
excluded. This filtering is performed using a Pandas DataFrame, where each column is accessed and a condition is applied to retain only those records where numMeasurements is greater than two. To visually represent the effect of this filtering, a graph (Figure 5) is plotted to show the relationship between the number of receivers and the number of data records. It is observed that 563,153 data records with fewer than 3 receivers are eliminated, leaving 485,422 records for further processing. After this filtration, the dataset is split into training and test subsets.

Aircraft transmit ADS-B and Mode S signals every two seconds. With 716 receivers deployed across a wide

geographic region at known locations, it is possible to receive these signals continuously from takeoff to landing. As a result, multiple data records can correspond to a single aircraft. Upon close examination of the dataset, it was observed that certain aircraft reported positions that deviated significantly from their expected trajectory. These abnormal positions are referred to as outliers. To eliminate such outliers, the training dataset is reprocessed using a Python-implementation of a rolling median filter. A latitude-longitude plot of one aircraft (Flight 1387) is generated to visualize its trajectory over time using the training dataset (Figure 6(a)), where outliers are clearly visible around 47.60° latitude.

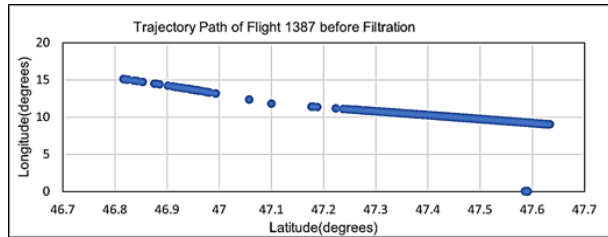


(a)

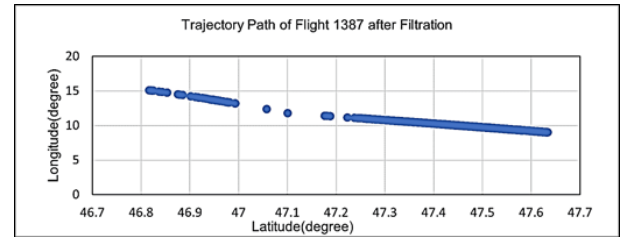


(b)

Figure 5. Number of Data records: (a) before filtration (b) after filtration.



(a)



(b)

Figure 6. Trajectory of Flight 1387 (a) before applying the median filter (b) after the median filter is applied.

The rolling median filter is then applied to smooth these extreme values, effectively aligning the trajectory with the aircraft's actual flight path (Pearson et al., 2016). The resulting filtered trajectory is shown in Figure 6(b). This same filtering approach is applied to all aircraft data within the training dataset. A final level of data filtration is performed based on aircraft altitude. The dataset contains two types of altitude measurements: barometric altitude (baro altitude), derived from the aircraft's onboard sensors, and geometric altitude (geo altitude), obtained from GPS-based positioning. Ideally, the baro and geo altitudes for each

aircraft should closely match. To verify this, a plot of baro altitude versus geo altitude for all aircraft is generated, as shown in Figure 7(a). It is observed that for two aircraft (IDs 1120 and 415), the baro and geo altitude values differ significantly. Therefore, data corresponding to these two aircraft are removed from the dataset, as illustrated in Figure 7(b). Once the data corresponding to the two aircraft is removed from the training dataset, the data is considered free of outliers and ready for training a machine learning algorithm. After applying all three filtration steps, a total of 386,589 data records remain in the training dataset.

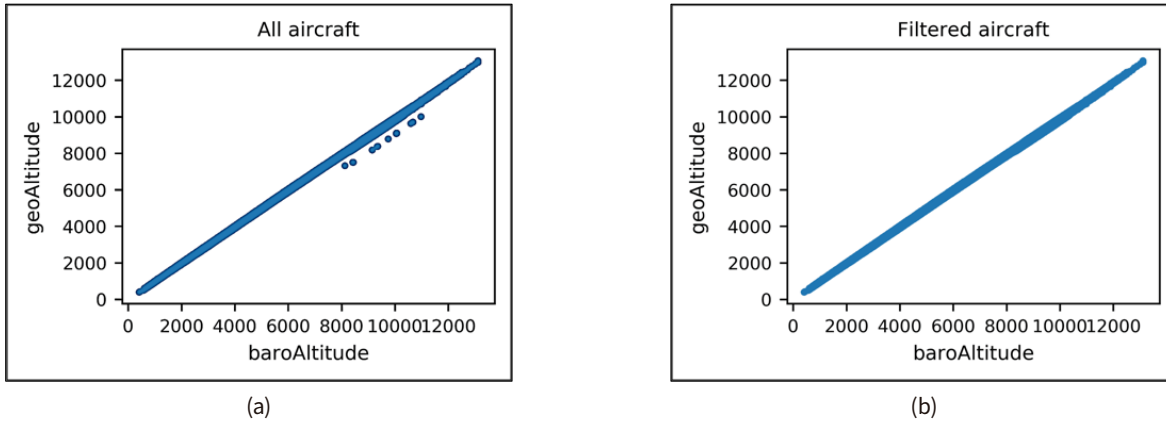


Figure 7. Geo Altitude versus Baro altitude of all Aircraft (a) before filtering (b) after filtering.

5.2 Position Estimation

Following the methodology outlined in Section 4, the KNN algorithm is applied to obtain initial estimates of latitude and longitude. Initially, K is set to 10, and the aircraft's position for each data record in the test dataset is estimated.

For example, the position estimates (latitude and longitude) for Flight 1428 over time are shown in Figure 8. The figure shows that the estimated positions form a trajectory representing Flight 1428's flight path. However, some position estimates deviate noticeably from this trajectory.

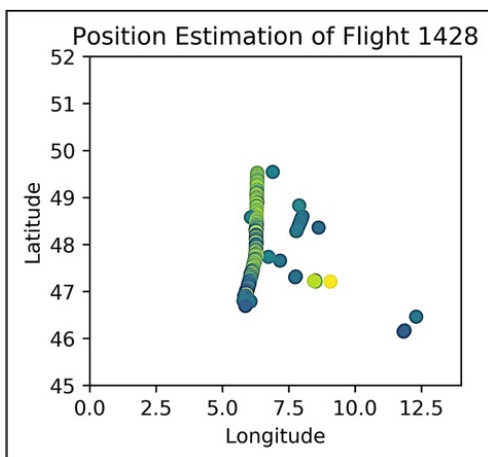


Figure 8. Position Estimation of Flight 1428.

To eliminate such erroneous position estimates, clustering algorithms are applied. The first level of filtering uses the Density-Based Spatial Clustering of Applications with Noise (DBSCAN) algorithm. DBSCAN groups estimates

that are spatially close together, based on a specified distance metric and a minimum number of neighboring points. Estimates that do not meet these criteria are classified as outliers.

A detailed explanation of this algorithm, along with the key parameters, is available in (Deng, 2020; Ester et al., 1996). For this work, the DBSCAN implementation from the scikit-learn library is used, with epsilon (ϵ) set to 0.05 and the minimum number of samples (min_samples) required to form a cluster set to 5. The dataset consists of spatially distributed aircraft position estimates that tend to form naturally well-separated, relatively uniform-density clusters. Preliminary experiments confirmed that these parameter values yielded clear, stable clustering results that aligned with the expected distribution of aircraft trajectories and effectively filtered out noise. Further parameter tuning did not yield a noticeable improvement in overall RMSE, indicating that the chosen configuration was both robust and optimal for this application. The position estimates for Flight 1428 after applying this filtering step are shown in Figure 9(a).

Following DBSCAN, a directional filter is applied to further refine the trajectory. This filter ensures that only those position points which align with the expected direction of flight are retained. Directional filtering is commonly used in trajectory estimation, motion tracking, or time-series analysis to eliminate data points that deviate significantly from the expected movement pattern. In this work, outliers are identified by computing the Euclidean distance between points within a window of three steps forward and backward. If the absolute difference between these distances exceeds a set threshold (5 meters), the point is considered an outlier and is removed. The outcome of this filtering step is shown in Figure 9(b).

Lastly, DBSCAN is reapplied—using the default parameters—to remove any residual trajectory points that remain off-course. The final trajectory after this step is illustrated in Figure 9(c). This three-step filtering process is applied to the estimated trajectories of all aircraft in the dataset to ensure robust and accurate removal of spurious position estimates.

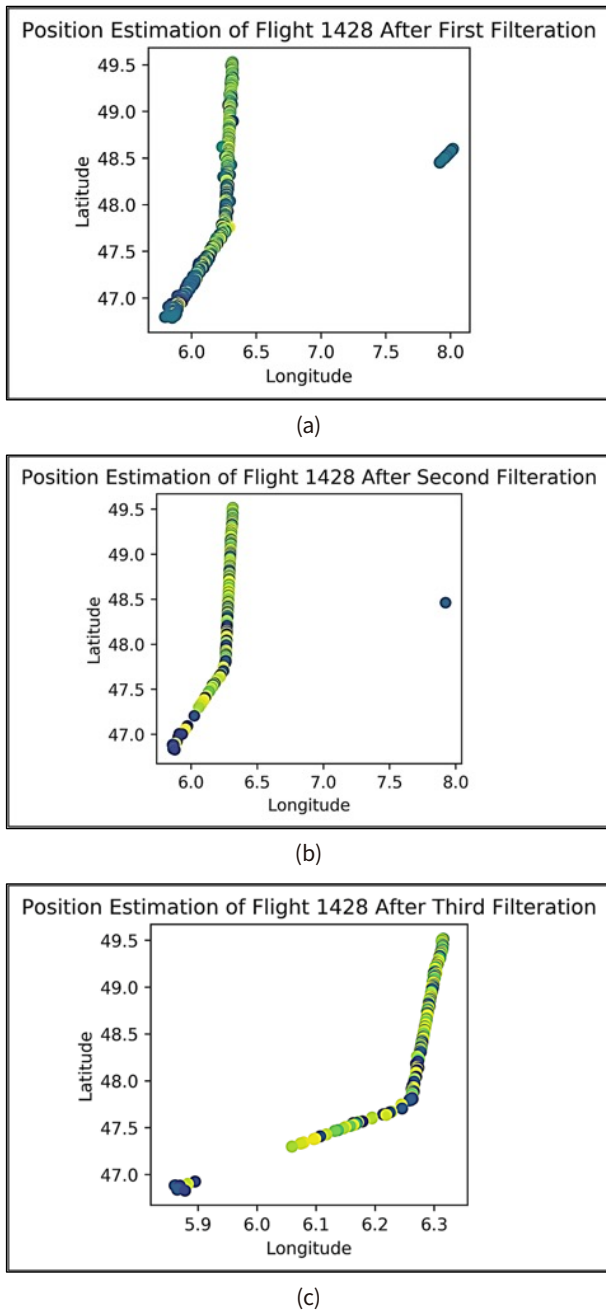


Figure 9. Filtration of estimated positions using (a) First DBSCAN filter (b) Direction filter (c) Second DBSCAN filter.

5.3 Validation of results

The OpenSky Network provides the true aircraft positions corresponding to each record in the testing dataset, serving as ground truth for evaluating the performance of the proposed algorithm. The estimated positions obtained using the proposed approach for each test data record are shown in Figure 10(a), while the corresponding actual positions from the OpenSky Network are illustrated in Figure 10(b). A comparison of these plots demonstrates the algorithm’s effectiveness in approximating true aircraft trajectories.

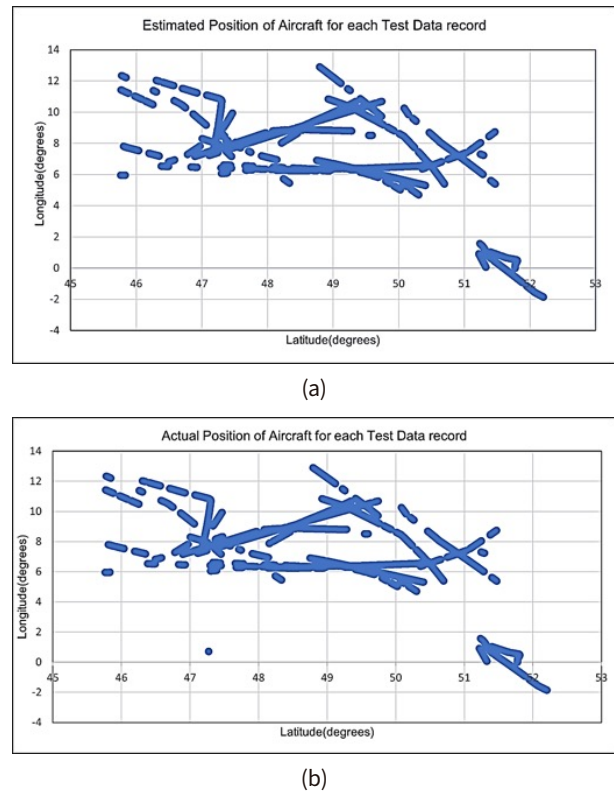


Figure 10. Aircraft positions (a) Estimated Positions; (b) Actual Positions.

Figure 10 illustrates the overall pattern of the estimated positions compared with the actual aircraft positions. To quantitatively assess the performance of the proposed algorithm, the Root Mean Square Error (RMSE) is computed for each estimated test data record relative to the corresponding ground truth. Both estimated and true position values, initially in degrees, are converted to Cartesian coordinates, and the Euclidean distance between them is calculated. The overall positional accuracy is

then derived by averaging the square root of the squared Euclidean distances across all test records. In the K-NN algorithm, the parameter K defines the number of nearest neighbors used to generate the initial position estimate. When K is set to 10, the proposed method achieves an average aircraft position estimation error of 39.4 meters. Additionally, a sensitivity analysis was performed to examine how the estimation accuracy varies with different values of K . The results of this experiment are summarized in Table 4.

Table 4. Accuracy of estimated locations for various K values.

K	RMSE (m)
5	42.18
10	39.414
15	38.90
20	38.6

Conclusions

Accurate aircraft positioning is necessary for efficient flight operations and safe air traffic management. The accuracy of position estimates provided by traditional methods, such as MLAT using TDOA, depends on the accuracy of the initial position estimate, which is essential for nonlinear optimization. The integration of multilateration with machine learning techniques offers a more realistic initial guess. In this paper, the results of aircraft position estimation using K-NN based Multilateration are presented. Real-time ADS-B data is obtained from the OpenSky network and split into test and training sets. A robust data preprocessing pipeline was implemented to improve the quality of input data. The k-NN algorithm was successfully implemented alongside multilateration, achieving an RMSE of 39.4m with a K value of 10. It is observed that even though the K value is increased beyond 10, the RMSE error remains the same. The results of this work highlight the efficacy of K-NN-based multilateration as an improved aircraft localization technique.

While the present work emphasizes a simple and interpretable approach, we recognize the potential advantages of more complex models. As part of our future work, we plan to explore advanced machine learning techniques, such as Random Forests (RF), Support Vector Regression (SVR), and neural networks, to improve positioning accuracy and scalability in more dynamic environments.

Acknowledgements

The research work presented in this paper is carried out as part of the objectives of the project sponsored by the Science and Engineering Research Board (SERB), Department of Science and Technology (DST), New Delhi, under the State University Research Excellence (SURE) scheme (SUR/2022/004990).

Funding

The authors received no specific funding for this work.

Conflict of Interest

The authors declare that they have no conflicts of interest to disclose.

References

- Adesina, D., Adagunodo, O., Dong, X., & Qian, L. (2019). Aircraft location prediction using deep learning. *Proceedings of the IEEE Military Communications Conference (MILCOM)*, 127-132.
<https://doi.org/10.1109/MILCOM47813.2019.9020888>
- Chen, J., Zhao, Y., Zhao, C., & Zhao, Y. (2018). Improved two-step weighted least squares algorithm for TDOA-based source localization. *Proceedings of the 19th International Radar Symposium*, 1-6.
<https://doi.org/10.23919/IRS.2018.8448149>
- Darabseh, A., Bitsikas, E., Tedongmo, B., & Pöpper, C. (2020). On ADS-B sensor placement for secure wide-area multilateration. *Proceedings*, 59(1), 3.
<https://doi.org/10.3390/proceedings2020059003>
- Deng, D. (2020). DBSCAN clustering algorithm based on density. *Proceedings of the 7th International Forum on Electrical Engineering and Automation (IFEAA)*, 949-953.
<https://doi.org/10.1109/IFEAA51475.2020.00199>
- Ester, M., Kriegel, H.-P., Sander, J., & Xu, X. (1996). A density-based algorithm for discovering clusters in large spatial databases with noise. *Proceedings of the Second International Conference on Knowledge Discovery and Data Mining (KDD'96)*, 226-231.
https://dl.acm.org/doi/10.5555/3001460.3001507?utm_source=chatgpt.com

- Figuet, B., Monstein, R., & Felux, M. (2020). Combined Multilateration with Machine Learning for Enhanced Aircraft Localization. *Proceedings*, 59(1), 2.
<https://doi.org/10.3390/proceedings2020059002>
- Ho, K. C., Lu, X., & Kovavisaruch, L. (2007). Source localization using TDOA and FDOA measurements in the presence of receiver location errors: Analysis and solution. *IEEE Transactions on Signal Processing*, 55(2), 684–696.
<https://doi.org/10.1109/TSP.2006.885744>
- Jin, B., Xu, X., & Zhang, T. (2018). Robust time-difference-of-arrival localization using weighted least squares with cone tangent plane constraint. *Sensors*, 18(3), 778.
<https://doi.org/10.3390/s18030778>
- Lee, H. B. (1975). A novel procedure for assessing the accuracy of hyperbolic multilateration systems. *IEEE Transactions on Aerospace and Electronic Systems*, AES-11(1), 2–15.
<https://doi.org/10.1109/TAES.1975.308023>
- Liu, Z., et al. (2018). A bias compensation method for distributed moving source localization using TDOA and FDOA with sensor location errors. *Sensors*, 18(11), 3747.
<https://doi.org/10.3390/s18113747>
- Lui, W. K., Chan, F. K. W., & So, H. C. (2009). Semidefinite programming approach for range-difference based source localization. *IEEE Transactions on Signal Processing*, 57(4), 1630–1633.
<https://doi.org/10.1109/TSP.2008.2010599>
- Monteiro, M., et al. (2015). Detecting malicious ADS-B broadcasts using wide area multilateration. *Proceedings of the IEEE/AIAA Digital Avionics Systems Conference (DASC)*, 4A3-1–4A3-12.
<https://doi.org/10.1109/DASC.2015.7311413>
- Pan, Y., Li, S., Li, B., et al. (2019). When UAVs coexist with manned airplanes: Large-scale aerial network management using ADS-B. *Transactions on Emerging Telecommunications Technologies*, 30, e3714.
<https://doi.org/10.1002/ett.3714>
- Pearson, R. K., Neuvo, Y., Astola, J., et al. (2016). Generalized Hampel filters. *EURASIP Journal on Advances in Signal Processing*, 87.
<https://doi.org/10.1186/s13634-016-0383-6>
- Peng, X., Chen, R., Yu, K., Ye, F., & Xue, W. (2020). An improved weighted k-nearest neighbor algorithm for indoor localization. *Electronics*, 9, 2117.
<https://doi.org/10.3390/electronics9122117>
- Ran, Q., Feng, R., Yu, N., & Wu, Y. (2016). A weighted least squares source localization algorithm using TDOA measurements in wireless sensor networks. *Proceedings of the 6th International Conference on Electronics Information and Emergency Communication*, 10–13.
<https://doi.org/10.1109/ICEIEC.2016.7589676>
- Rayapu, M. K., Talari, S., & Darshini, G. I. P. (2017). Multilateration with ADS-B: A boon in civil aviation application. *Proceedings of the International Conference on Electrical, Electronics, Communication, Computer, and Optimization Techniques (ICECCOT)*, 1–6.
<https://doi.org/10.1109/ICECCOT.2017.8284565>
- Shen, J., Molisch, A. F., & Salmi, J. (2012). Accurate passive location estimation using TOA measurements. *IEEE Transactions on Wireless Communications*, 11(6), 2182–2192.
<https://doi.org/10.1109/TWC.2012.040412.110697>
- Strohmeier, M., Lenders, V., & Martinovic, I. (2015). On the security of the automatic dependent surveillance-broadcast protocol. *IEEE Communications Surveys & Tutorials*, 17(2), 1066–1087.
<https://doi.org/10.1109/COMST.2014.2365951>
- Strohmeier, M., Martinovic, I., & Lenders, V. (2018). A k-NN-based localization approach for crowdsourced air traffic communication networks. *IEEE Transactions on Aerospace and Electronic Systems*, 54(3), 1519–1529.
<https://doi.org/10.1109/TAES.2018.2797760>
- Tekdas, O., & Isler, V. (2010). Sensor placement for triangulation-based localization. *IEEE Transactions on Automation Science and Engineering*, 7(3), 681–685.
<https://doi.org/10.1109/TASE.2009.2037135>
- Torrieri, D. J. (1984). Statistical theory of passive location systems. *IEEE Transactions on Aerospace and Electronic Systems*, AES-20(2), 183–197.
<https://doi.org/10.1109/TAES.1984.310439>
- Wang, D., Zhao, X., & Li, Y. (2025). Fingerprint localization based on hybrid TOA, AOA, and RSS measurements. *Discover Applied Sciences*.
<https://doi.org/10.1007/s42452-025-06462-y>
- Weinstein, E. (1982). Optimal source localization and tracking from passive array measurements. *IEEE Transactions on Acoustics, Speech, and Signal Processing*, 30(1), 69–76.
<https://doi.org/10.1109/TASSP.1982.1163855>

Wu, P., Su, S., Zuo, Z., Guo, X., Sun, B., & Wen, X. (2019). Time difference of arrival localization combining weighted least squares and firefly algorithm. *Sensors*, 19(11), 2554.
<https://doi.org/10.3390/s19112554>

Xu, J., Ma, M., & Law, C. L. (2006). Position estimation using UWB TDOA measurements. *Proceedings of the IEEE International Conference on Ultra-Wideband*, 605–610.
<https://doi.org/10.1109/ICU.2006.281617>

Yu, F., Zhang, Q., Yu, W., Maharjan, S., & Zhang, Y. (2014). An improved k-nearest neighbor algorithm for localization in multipath environments. *EURASIP Journal on Wireless Communications and Networking*, 208.
<https://doi.org/10.1186/1687-1499-2014-208>

Zweck, J. (2016). Analysis of methods used to reconstruct the flight path of Malaysia Airlines flight 370. *SIAM Review*, 58, 555–574.
<https://doi.org/10.1137/140991996>